Early Astigmatism Can Alter Myopia Development in Chickens

Sonal Aswin Vyas and Chea-su Kee

School of Optometry, The Hong Kong Polytechnic University, Hong Kong SAR, China

Correspondence: Chea-su Kee, School of Optometry, The Hong Kong Polytechnic University, Hong Kong SAR, China; c.kee@polyu.edu.hk.

PURPOSE. To determine the effects of optically imposed astigmatism on myopia development in chickens.

METHODS. Chicks were randomly assigned to wear either spherical ($-10D$, "LIM", $n = 14$) or sphero-cylindrical lenses ($n \geq 19$ in each group) monocularly for a week from 5 days of age. All lenses imposed the same magnitude of spherical-equivalent hyperopic defocus ($-10D$), with the two astigmatic magnitudes ($-8D$ or $-4D$) and four axes (45°, 90°, 135°, or 180°) altered to simulate four subtypes of clinical astigmatism. At the end of the treatment, refractive state was measured for all birds, whereas ocular axial dimensions and corneal curvature were measured for subsets of birds.

RESULTS. Sphero-cylindrical lens wear produced significant impacts on nearly all refractive parameters ($P < 0.001$), resulting in myopic-astigmatic errors in the treated eyes. Compared to LIM, the presence of astigmatic blur induced lower myopic error (all except L180 group, $P < 0.001$) but with higher refractive astigmatism (all $P < 0.001$) in birds treated with sphero-cylindrical lenses. Distributions of the refractive, axial, and corneal shape parameters in the sphero-cylindrical lens-wear groups indicated that the astigmatic blur had directed the eye growth toward the least hyperopic image plane, with against-the-rule (ATR) and with-the-rule (WTR) astigmatisms typically inducing differential biometric changes.

CONCLUSIONS. The presence of early astigmatism predictably altered myopia development in chicks. Furthermore, the differential effects of WTR and ATR astigmatisms on anterior and posterior segment changes suggest that the eye growth mechanism is sensitive to the optical properties of astigmatism.

Keywords: myopia development, astigmatism, chicken

Astigmatism is a highly prevalent refractive error worldwide, frequently coexisting with myopia (near-/short-sightedness) and hyperopia (far-/long-sightedness).[1–3] The prevalence of astigmatism in school-aged children is generally higher in East Asian populations (18.4%–42.7%)[4–8] than in other ethnicities (3.5%–9.5%).[9–12] Several studies involving multiethnic populations have also reported a significantly higher prevalence of astigmatism in residents of Asian[13] and East Asian origin.[14,15] The association of astigmatism with increasing myopia in school-age Asian populations, including Hong Kong Chinese, raises the question of whether the presence of early astigmatism contributes to the development of myopia.[6,8,16,17] Similar to the majority of epidemiologic studies, astigmatism in Hong Kong Chinese school-age children is related to spherical errors (i.e., myopia and hyperopia), corneal in nature, and predominantly with-the-rule (WTR), in which the vertical meridian has stronger refractive power than the horizontal meridian.[6,8,18] Because of the optical aberration, patients with astigmatism have degraded vision that can be improved only by ophthalmic aids or corneal surgery. Significant astigmatism has been associated with abnormalities in retinal electrophysiology,[19] amblyopia,[20,21] and permanent visual deficits in grating acuity,[22–24] visual acuity,[23,25] contrast sensitivity,[22,24] and stereopsis.[22,24] Alarmingly, in a population of school-age children with a high prevalence of significant astigmatism, early intervention with cylindrical spectacle lenses improved visual function (grating and vernier acuities) only in the first 6 weeks of lens wear, as their visual function measured after 1 year of treatment was still lower than that of nonastigmatic children.[26] Despite the high prevalence and the multiple visual impairments associated with astigmatism in school-age children, there is no consensus among clinical practitioners as to when astigmatism should be corrected in young children.[27]

The axis orientation of astigmatism has been associated with ametropia development. In particular, previous studies have shown that children with against-the-rule (ATR) astigmatism, in which the horizontal meridian has stronger refractive power than vertical meridian, were more likely to become myopic compared to those who had WTR astigmatism.[28–30] In addition, analysis of the relationship between astigmatic axis and ametropia in patients from a large optometry practice revealed that high myopes and low myopes have increased odds of WTR and ATR astigmatism, respectively.[31] A recent study in young adults also showed a high prevalence of WTR astigmatism in subjects with high myopia or hyperopia,[32] and a similar

association has been reported in the Hong Kong Chinese clinical population.[8] While long-term, longitudinal studies are lacking to confirm the pattern of change in ocular components during the course of astigmatic development, the disappearance of infantile astigmatism before school age has led to the hypothesis that astigmatism acts as a visual error signal during early eye growth. It has been proposed that the presence of astigmatism may improve the efficiency of the mechanism that regulates emmetropization by integrating the optical signals associated with the two principal power meridians of astigmatic eyes.[33,34] Alternatively, it has been suggested that astigmatism may come about as a consequence of ametropic development,[31] or the two may share a common etiology.[3]

To date, the impact of astigmatism on refractive development has been studied only in monkeys[35,36] and chicks.[37–42] However, the important question of whether and how the presence of early astigmatism can alter the endpoint of myopia development has not been answered. This study tested this hypothesis using a chick model wearing sphero-cylindrical lenses imposing hyperopic-astigmatic blur. The effects on refractive, axial, and corneal components were measured after a week and compared to a control group wearing spherical lenses imposing the same magnitude of spherical equivalent errors but no astigmatic error. It was found that the presence of astigmatism altered the endpoints of myopia development in chicks depending on the astigmatic properties.

MATERIALS AND METHODS

Animals

In total, 193 White Leghorn chicks (*Gallus gallus domesticus*) were obtained from the Centralized Animal Facility of the Hong Kong Polytechnic University. They were reared in the animal facility in a 12-hour/12-hour light/dark cycle (lights on from 0700 to 1900) under controlled temperature (20−22°C) with unlimited access to food and water. The illumination level was about 150 lux at the chick's eye level. Care and use of animals were in compliance with the ARVO Statement for the Use of Animals in Ophthalmic and Vision Research. The experimental protocol was reviewed and approved by the Animal Subjects Ethics subcommittee of the Hong Kong Polytechnic University (ASESC#15-16/41).

Visual Manipulations

On posthatching day 5 (P5), chicks were randomly assigned to wear either spherical (−10D, $n = 14$) or sphero-cylindrical lenses ($n = 179$) of identical spherical-equivalent power (−10D) on the right eye for 7 days (P5–P12); the left eye was left untreated. Previous studies have shown that the mechanism regulating eye growth in chicks is sensitive to spherical defocus of −10D to +20D[43,44] within a short period of time and with less intersubject variability when compared to the ocular responses induced by form deprivation myopia. In addition, obvious refractive and axial dimensional changes (see also Table 3) have consistently been reported in previous studies using the −10D LIM paradigm[41,43,45]; we thus selected −10D spherical defocus to induce myopia development in this study. We adopted the same starting point of lens treatment (P5) as our previous study[41] to minimize the potential optical effects of the naturally occurring astigmatism in chicks[39,46] from interfering with the astigmatism

imposed by the sphero-cylindrical lens. To determine the effects of astigmatism on myopia development, a total of eight combinations of hyperopic-astigmatic defocus were employed: two astigmatic magnitudes (−4DC or −8DC) and four axes (45°, 90°, 135°, or 180°) were imposed using two sphero-cylindrical lenses (low magnitude = −8DS/−4DC; high magnitude = −6DS/−8DC). Each of these eight treatment groups was denoted with a letter indicating the astigmatic magnitude (H, high; L, low), followed by a number indicating the astigmatic axis (e.g., H45). Table 1 describes how the different refractive conditions were achieved by four of these eight combinations imposing the higher magnitude of astigmatic errors (−8DC). Note that the two principal powered meridians had −6D and −14D, respectively, imposing astigmatic magnitude of 8DC and spherical equivalent of −10D. All lenses (PMMA material, base curve = 7.5mm, diameter = 10.8 mm, optical zone = 10 mm; Conforma, VA, USA) were first verified for power using a digital focimeter (Auto Lensmeter LM-1800PD/1800P; Nidek Co., Japan). Each lens was glued firmly to a Velcro ring using Norland Optical adhesive (Norland Products, New Brunswick, NJ, USA), and the axis of the negative cylinder (i.e., the least negative-power meridian) was labeled clearly with a fine-tip marker on each side of the ring. The Velcro mate was then glued to the feathers around the right orbit for the attachment of the Velcro ring with the lens, and the space between the hooks and loops of this Velcro mating pair ensured enough air ventilation to prevent a foggy lens. To accurately orient the axis of the negative cylinder, a protractor was used to mark the intended treatment axis on this Velcro mate attached to the feathers by referring to the palpebral fissure as the horizontal reference line (0° or 180°). By matching the line on the Velcro ring (with lens) and the line on the Velcro mate (on the feathers), the accuracy of the cylindrical axis could be controlled within ±5°. During the treatment period (P5−P12), lenses were cleaned frequently and checked for any scratches or defects, and all lenses with defects were replaced immediately. If the lens was found detached during the treatment period, the data were excluded from further analysis.
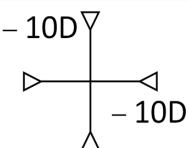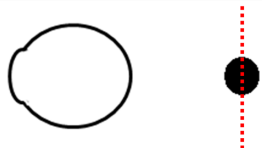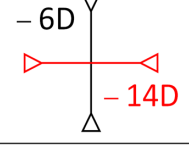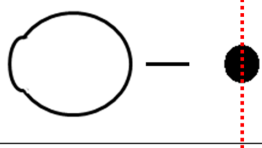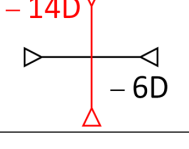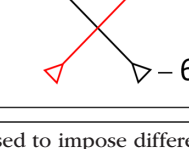
Measurement

At the end of the treatment period, refractive state, corneal curvature, and ocular axial dimensions were measured by a modified Hartinger coincidence refractometer[47] (Jena coincidence Refractometer, Model 110; Carl Zeiss Meditec, Jena, Germany), custom-made Placido-ring videokeratography,[48] and high-resolution A-scan ultrasonography,[49,50] respectively. The refractive state was measured for all birds, whereas corneal curvature and ocular axial dimensions were measured for subsets of birds. All measurements were performed in the morning, within a ±1-hour time frame to avoid any variation due to diurnal rhythms.[49]

Hartinger Coincidence Refractometer

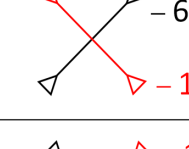After the animal was anesthetized using isoflurane (1.0%–1.5% in oxygen), the palpebral fissure was aligned horizontally and the eye was held open using a lid retractor (tooth-proof stainless steel wire; American Fishing, Coatesville, PA, USA). The lid retractor was inserted gently so that it did not come into contact with the cornea and distort the mires as described in a previous study.[41] The presence of a lid retractor and anesthesia did not prevent the

TABLE 1. Optically Imposed Hyperopic-Astigmatic Defocus Conditions

Refractive Conditions	Lens Treatments	Lens Effects on Image/s
High hyperopia	−10D / −10D	
Hyperopia + WTR (90°)	−6D / −14D	
Hyperopia + ATR (180°)	−14D / −6D	
Hyperopia + Oblique	−6D / −14D	
	−14D / −6D	Eye -6D COLC -14D

Spherical and sphero-cylindrical lenses were used to impose different refractive conditions. Left: refractive conditions imposed; middle: pictorial representation of principal power meridians of spherical lens and sphero-cylindrical lenses of high astigmatic magnitude; right: optical effects on image properties of a point source. Note that all refractive conditions imposed identical spherical-equivalent errors (−10D), as indicated by the identical locations of circle of least confusion (blurred circle aligned with red dashed line).

eye from blinking through the nictitating membrane (the "third eyelid"), allowing corneal hydration and optical clarity to be maintained during the measurement (2–3 minutes per eye). Three measurements for both principal meridians were recorded and averaged using power vector analysis.[51] Refractive components used for further analysis included spherical-equivalent refractive error (M), refractive astigmatism (RA), least myopic meridian (LMM), most myopic meridian (MMM), and the two astigmatic components, R-J0 and R-J45.[51]

Placido Ring Videokeratography System

A Placido ring–based videokeratography system was used to measure corneal curvature in alert chicks. Once the pupil was aligned concentrically with the Placido rings, the CCD camera captured 500–800 frames via multiple-shot mode. Six high-quality images with complete Placido ring images were selected manually for each eye, based on the pupil alignment and diameter.[48] These images were analyzed using a custom-written MATLAB algorithm to obtain corneal curvatures of the principal meridians. These parameters were used to derive corneal shape parameters using power vector analysis: average corneal radius (CR), flattest curvature (FCR), steepest curvature (SCR), corneal astigmatism (CA), and the two astigmatic components, C-J0 and C-J45. Likewise, the refractive components of internal astigmatism were calcu-

lated by subtracting corneal shape parameters from refractive parameters.

A-Scan Ultrasonography

High-resolution A-scan ultrasonography consisted of a 50-MHz focused polymer with a manually adjustable pulser-receiver (model 176599; Panametrics), employing sampling signals at 500 MHz. Eyelids of anesthetized chicks were held open with a speculum while three measurements were taken along the pupillary axis. Each measurement consisted of 50 echograms, and these were averaged as previously described[49,50] to obtain the axial dimensions of individual ocular components. The axial length was defined as the sum of the distance from anterior cornea to the posterior sclera.

Statistical Analysis

Data were analyzed using SPSS statistical software (version 23.0.0; IBM, Chicago, IL, USA). The effect of lens wear on biometric parameters was first tested by comparing the treated and fellow untreated eyes using paired *t*-tests. To test the effect of the presence of astigmatism on myopia development, one-way ANOVAs with Bonferroni's pairwise post hoc comparisons were used to compare parameters across all nine groups of birds (spherical and sphero-cylindrical lenses). To test the effect of characteristics of

astigmatism on ocular biometric parameters, two-way ANOVAs (first factor: astigmatic magnitude, two levels; second factor: astigmatic axis, four orientations) followed by Bonferroni's multiple post hoc comparisons were used to compare the eight groups of birds treated with sphero-cylindrical lenses. Pearson correlation analyses were performed for refractive, corneal, and axial parameters. In all tests, the significance level was set at the 95% level of confidence. Unless otherwise stated, all data were expressed in terms of mean ± SE.

Results

Effects of Visual Manipulations on Treated Eyes

Refractive Parameters. At the end of the 7-day treatment period (P12), all nine visual manipulations produced significant impacts on virtually all refractive parameters of the treated eyes (Table 2). Wearing −10D spherical lenses (LIM) induced significant changes in all refractive parameters except R-J45 (paired *t*-tests, all $P < 0.01$). Similarly, all eight groups that received sphero-cylindrical-lens treatment showed significant changes in most refractive parameters in the treated eyes (all $P < 0.001$); only the two groups treated with the axis oriented at 180° (H180 and L180) showed nonsignificant change in both vector components (R-J0 and R-J45) in the treated eyes.

Axial Parameters. Table 3 shows a comparison of ocular axial dimensions between treated and fellow eyes. Individual treatments resulted in a thinner cornea (H45, H180, and L180, paired *t*-tests, all $P < 0.05$), a thinner crystalline lens (H90, $P < 0.05$), a deeper anterior chamber, (all groups, all $P < 0.05$), a deeper vitreous chamber, and a longer axial length (all groups, all $P < 0.01$). Interestingly, while wearing −10D spherical lens induced a thinner choroid as reported in previous studies (paired *t*-test, $P < 0.01$), wearing sphero-cylindrical lenses induced a thicker choroid with statistical significance in all (paired *t*-test, $P < 0.01$) except H90, L90, and L135 groups (thicker choroid but did not reach statistical significance).

Corneal Shape Parameters. The effects of spherical and sphero-cylindrical lens wear on corneal shape parameters were in general less pronounced than those on refractive parameters. As presented in Table 4, significantly higher corneal astigmatisms were observed in the treated eyes of LIM, L45, H90, L90, H135, and L135 groups compared to the fellow untreated eyes (paired *t*-test, all $P < 0.05$). In contrast, wearing a sphero-cylindrical lens induced a steeper cornea (SCR and CR) in the L180 group but a flatter cornea (FCR and CR) in the H135 group when compared to their fellow eyes (all $P < 0.05$).

Effects of Presence Versus Absence of Astigmatism on Myopia Development

Refractive Parameters. Compared to spherical lens wear, the presence of astigmatic blur imposed by sphero-cylindrical lens wear induced less myopic errors (Fig. 1A and Supplementary Table S1) in the treated eyes. Figure 1A shows the frequency distributions of spherical equivalent (top), the least myopic meridian (middle), and the most myopic meridian (bottom) in treated eyes receiving different magnitudes (left: high cylinder, 8DC; right: low cylinder, 4DC) and axes (yellow: 45°; blue: 90°; green: 135°; red: 180°). In each plot, the boxplot represents the data of

−10D lens-wearing chicks, and the two dashed lines mark the locations of line focus with magnitudes corresponding to the sphero-cylindrical lens-wear chicks. Compared to −10D group, groups treated with sphero-cylindrical lenses developed significantly lower M (all except L180 group; one-way ANOVA with Bonferroni's post hoc tests, all $P \leq 0.01$), LMM (all except L180 group; one-way ANOVA with Bonferroni's post hoc tests, all $P < 0.001$), and MMM (H45, H90, and H135; one-way ANOVA with Bonferroni's post hoc tests, all $P < 0.05$). The presence of astigmatic blur with sphero-cylindrical lens wear also induced significantly higher refractive astigmatism in all groups (one-way ANOVAs with Bonferroni's post hoc tests, all $P < 0.001$; Supplementary Table S1) and had significant impacts on the two vector components (one-way ANOVAs, all $P < 0.001$): compared to the −10D group, higher R-J0 (L45, H90, L90, H135, and L135; Bonferroni's post hoc tests, all $P \leq 0.01$) and higher R-J45 (H45, L45, and H135; Bonferroni's post hoc tests, all $P < 0.01$) were found in individual sphero-cylindrical lens-wear groups (Supplementary Table S1).

Axial Parameters. Sphero-cylindrical lens wear had a significant impact on corneal thickness, vitreous chamber depth, and choroidal thickness when compared to −10D lens wear (Supplementary Table S2). Figure 1B shows frequency distributions of corneal thickness (top), vitreous chamber depth (middle), and choroidal thickness (bottom) in eyes treated by sphero-cylindrical lens wear. Compared to the −10D group, individual groups treated with sphero-cylindrical lenses had thicker central corneal thickness (L45, H90, L135, and L180; one-way ANOVAs with Bonferroni's post hoc tests, all $P \leq 0.05$), shorter vitreous chamber depth (H45, L90, and H180; one-way ANOVAs with Bonferroni's post hoc tests, all $P < 0.05$), and thicker choroidal thickness (H45, L45, H135, and L180; one-way ANOVAs with Bonferroni's post hoc tests, all $P < 0.05$). There were no significant differences in the remaining axial components (anterior chamber depth [ACD], lens thickness [LT], retinal thickness [RT], scleral thickness [ST], and axial length [AXL]).

Corneal Shape Parameters. Sphero-cylindrical lens wear did not result in a significant effect on the majority of corneal shape parameters when compared to −10D lens wear (Supplementary Table S3); the only exception was a more positive C-J45 in both H45 and L45 groups (one-way ANOVA with Bonferroni's post hoc tests, $P < 0.01$).

Effects of Astigmatic Characteristics on Myopia Development

Refractive Parameters. The impacts of characteristics of astigmatism (i.e., orientation and magnitude) on myopia development were tested among the eight groups of birds receiving sphero-cylindrical lens wear. While astigmatic orientation had significant main effects on all six refractive parameters (M, LMM, MMM, RA, R-J0, and R-45; two-way ANOVAs, all $P < 0.01$), astigmatic magnitude showed a significant impact on three spherical components (M, LMM, and MMM; two-way ANOVAs, all $P < 0.001$). In addition, significant interaction effects of astigmatic axis with magnitude were observed on RA and R-J45 (two-way ANOVAs, both $P < 0.05$). Figure 2 shows three parameters (two refractive and one axial) that were affected the most by the characteristics of sphero-cylindrical lens wear. As shown in Figure 2A, both H180 and L180 groups developed significantly more myopic LMM compared to the other

TABLE 2. Effects of Spherical and Sphero-Cylindrical Lens Wear on Refractive Parameters in Treated Eyes

Refractive (D)	Group (n)	45 (≥19) RE	45 (≥19) LE	90 (22) RE	90 (22) LE	135 (≥21) RE	135 (≥21) LE	180 (≥22) RE	180 (≥22) LE	−10DS (14) RE	−10DS (14) LE
M	H	−5.84 ± 0.35***	−0.36 ± 0.10	−5.97 ± 0.36***	−0.83 ± 0.14†††	−5.66 ± 0.36***	−0.51 ± 0.10	−7.56 ± 0.73***	−0.75 ± 0.17††	−10.29 ± 0.22***	−0.06 ± 0.07
	L	−7.71 ± 0.45***	−0.44 ± 0.08	−6.91 ± 0.40***	−0.60 ± 0.12	−6.63 ± 0.41***	−0.24 ± 0.08	−8.85 ± 0.58***	−0.63 ± 0.10†		
LMM	H	−4.43 ± 0.37***	−0.28 ± 0.10	−4.18 ± 0.34***	−0.79 ± 0.13†††	−4.12 ± 0.36***	−0.44 ± 0.10	−6.77 ± 0.72***	−0.64 ± 0.16††	−10.06 ± 0.24***	−0.02 ± 0.08
	L	−5.88 ± 0.47***	−0.39 ± 0.08	−5.35 ± 0.45***	−0.48 ± 0.11	−5.11 ± 0.41***	−0.19 ± 0.07	−7.89 ± 0.54***	−0.52 ± 0.09		
MMM	H	−7.24 ± 0.36***	−0.43 ± 0.10	−7.85 ± 0.45***	−0.94 ± 0.15†††	−7.20 ± 0.38***	−0.58 ± 0.11	−8.37 ± 0.75***	−0.82 ± 0.19††	−10.51 ± 0.20***	−0.10 ± 0.07
	L	−8.46 ± 0.44***	−0.50 ± 0.08	−8.46 ± 0.36***	−0.64 ± 0.13	−8.15 ± 0.42***	−0.30 ± 0.08	−9.94 ± 0.62***	−0.74 ± 0.11†		
RA	H	−2.82 ± 0.19***	−0.14 ± 0.04	−3.67 ± 0.23***	−0.15 ± 0.05	−3.08 ± 0.17***	−0.15 ± 0.03	−1.62 ± 0.12***	−0.18 ± 0.06	−0.46 ± 0.08**	−0.09 ± 0.03
	L	−2.57 ± 0.13***	−0.11 ± 0.03	−3.10 ± 0.20***	−0.16 ± 0.04	−3.04 ± 0.13***	−0.12 ± 0.03	−2.06 ± 0.21***	−0.22 ± 0.05		
R-J0	H	−0.86 ± 0.15***	−0.07 ± 0.02	−1.50 ± 0.18***	−0.06 ± 0.02	−1.28 ± 0.07***	−0.07 ± 0.01	+0.20 ± 0.16	−0.09 ± 0.03	−0.20 ± 0.04**	−0.04 ± 0.01
	L	−1.06 ± 0.07***	−0.05 ± 0.01	−1.39 ± 0.13***	−0.07 ± 0.02	−1.41 ± 0.06***	−0.06 ± 0.01	−0.13 ± 0.22	−0.10 ± 0.02		
R-J45	H	+0.91 ± 0.10***	+0.00 ± 0.01	+0.33 ± 0.10**	+0.00 ± 0.01	−0.65 ± 0.13***	+0.00 ± 0.00	+0.03 ± 0.09	−0.01 ± 0.01	−0.02 ± 0.03	−0.01 ± 0.00
	L	+0.66 ± 0.07***	+0.00 ± 0.00	+0.23 ± 0.09**	−0.01 ± 0.00	−0.27 ± 0.10**	−0.01 ± 0.00	−0.07 ± 0.09	+0.01 ± 0.01		

Comparisons of six refractive parameters between treated right eyes (RE) versus the untreated left eyes (LE) by student paired t-tests and across fellow untreated left eyes from the −10DS group versus fellow untreated left eyes from the eight sphero-cylindrical lens-wear groups using one-Way ANOVA with Bonferroni's post hoc tests. Data for groups treated with sphero-cylindrical lenses were arranged according to the astigmatic axis (45°, 90°, 135°, and 180°) and magnitude (high, H, −6DS/−8DC; low, L, −8DS/−4DC). Data for group treated with spherical lenses (−10DS) are presented on the right for easy comparison. The levels of significance are represented by different symbols: *P < 0.05, **P < 0.01, and ***P < 0.001 for paired t-tests and †P < 0.05, ††P < 0.01, and †††P < 0.001 for post hoc tests.

Investigative Ophthalmology & Visual Science

TABLE 3. Effects of Spherical and Sphero-Cylindrical Lens Wear on Axial Parameters in Treated Eyes

Groups (n)		45 (≥13) RE	LE	90 (≥13) RE	LE	135 (≥18) RE	LE	180 (≥13) RE	LE	−10DS (14) RE	LE
CCT (µm)	H	186.2 ± 3.05*	190.6 ± 2.39	189.4 ± 3.08	194.8 ± 4.31†	183.7 ± 1.66	185.4 ± 2.01	186.5 ± 2.61*	198.1 ± 4.60††	175.5 ± 2.62	178.1 ± 2.99
	L	190.4 ± 3.07	190.3 ± 2.55	186.2 ± 3.08	194.2 ± 3.62	189.9 ± 2.80	188.5 ± 2.84	189.5 ± 2.47***	203.6 ± 4.21†††		
ACD (mm)	H	1.28 ± 0.02***	1.19 ± 0.02	1.29 ± 0.03***	1.15 ± 0.02†	1.28 ± 0.02**	1.21 ± 0.01	1.34 ± 0.04**	1.17 ± 0.02	1.35 ± 0.03**	1.26 ± 0.02
	L	1.29 ± 0.03*	1.21 ± 0.02	1.32 ± 0.03**	1.21 ± 0.02	1.28 ± 0.02***	1.21 ± 0.01	1.32 ± 0.02***	1.14 ± 0.03†††		
LT (mm)	H	2.07 ± 0.01	2.06 ± 0.02	2.05 ± 0.02*	2.08 ± 0.02	2.07 ± 0.02	2.09 ± 0.02	2.08 ± 0.02	2.08 ± 0.02	2.06 ± 0.02	2.07 ± 0.02
	L	2.07 ± 0.01	2.07 ± 0.02	2.07 ± 0.02	2.05 ± 0.02	2.06 ± 0.01	2.06 ± 0.01	2.08 ± 0.03	2.10 ± 0.03		
VCD (mm)	H	5.40 ± 0.03***	5.13 ± 0.03	5.42 ± 0.04***	5.11 ± 0.04	5.48 ± 0.04***	5.15 ± 0.03	5.35 ± 0.05***	5.11 ± 0.04	5.58 ± 0.02***	5.18 ± 0.02
	L	5.53 ± 0.05***	5.24 ± 0.04	5.33 ± 0.05***	5.06 ± 0.04	5.50 ± 0.04***	5.17 ± 0.02	5.42 ± 0.03***	5.12 ± 0.04		
RT (mm)	H	0.25 ± 0.00	0.26 ± 0.01	0.25 ± 0.00	0.25 ± 0.00	0.25 ± 0.00*	0.26 ± 0.00†	0.25 ± 0.01*	0.24 ± 0.01	0.23 ± 0.01	0.23 ± 0.01
	L	0.24 ± 0.01	0.25 ± 0.01	0.25 ± 0.01	0.26 ± 0.01	0.25 ± 0.00	0.25 ± 0.00	0.25 ± 0.01*	0.26 ± 0.01		
CT (mm)	H	0.23 ± 0.01**	0.21 ± 0.01	0.22 ± 0.01	0.20 ± 0.01	0.23 ± 0.01**	0.20 ± 0.01	0.23 ± 0.00**	0.21 ± 0.01	0.19 ± 0.01**	0.20 ± 0.00
	L	0.23 ± 0.01***	0.20 ± 0.01	0.22 ± 0.01	0.21 ± 0.01	0.20 ± 0.01	0.19 ± 0.01	0.23 ± 0.01**	0.21 ± 0.01		
ST (mm)	H	0.12 ± 0.00*	0.10 ± 0.01†	0.11 ± 0.01	0.10 ± 0.01	0.12 ± 0.01	0.11 ± 0.00	0.12 ± 0.00	0.10 ± 0.01	0.12 ± 0.00	0.13 ± 0.00
	L	0.12 ± 0.01*	0.11 ± 0.00	0.12 ± 0.00	0.12 ± 0.01	0.13 ± 0.01**	0.11 ± 0.01	0.11 ± 0.00*	0.10 ± 0.01		
AXL (mm)	H	9.54 ± 0.04***	9.13 ± 0.03	9.53 ± 0.05***	9.08 ± 0.04	9.61 ± 0.04***	9.21 ± 0.03	9.56 ± 0.08**	9.10 ± 0.05	9.71 ± 0.02***	9.25 ± 0.02
	L	9.68 ± 0.06***	9.27 ± 0.05	9.50 ± 0.07***	9.09 ± 0.06	9.61 ± 0.04***	9.18 ± 0.03	9.58 ± 0.03***	9.13 ± 0.05		

Comparisons of eight axial parameters were made for treated right eyes (RE) versus the untreated left eyes (LE) by student paired t-tests and for fellow untreated left eyes from the −10DS group versus fellow untreated left eyes from the eight sphero-cylindrical lens-wear groups using one-Way ANOVA with Bonferroni's post hoc tests. Data for groups treated with sphero-cylindrical lenses were arranged according to the astigmatic axis (45°, 90°, 135°, and 180°) and magnitude (high, H, −6DS/−8DC; low, L, −8DS/−4DC). Data for group treated with spherical lenses (−10DS) are presented on the right for easy comparison. CCT, central corneal thickness; CT, choroidal thickness. The levels of significance are represented by different symbols: *$P < 0.05$, **$P < 0.01$, and ***$P < 0.001$ for paired t-tests and †$P < 0.05$, ††$P < 0.01$, and †††$P < 0.001$ for post hoc tests.

TABLE 4. Effects of Spherical and Sphero-Cylindrical Lens Wear on Corneal Shape Parameters in Treated Eyes

Groups (n)		45 (≥13) RE	45 (≥13) LE	90 (≥13) RE	90 (≥13) LE	135 (≥18) RE	135 (≥18) LE	180 (≥13) RE	180 (≥13) LE	−10DS (14) RE	−10DS (14) LE
FCR (mm)	H	3.15 ± 0.02	3.13 ± 0.01	3.17 ± 0.03	3.17 ± 0.02	3.21 ± 0.02*	3.18 ± 0.01	3.16 ± 0.03	3.16 ± 0.02	3.15 ± 0.01	3.16 ± 0.01
	L	3.21 ± 0.02	3.21 ± 0.02	3.14 ± 0.03	3.13 ± 0.02	3.19 ± 0.02	3.18 ± 0.02	3.14 ± 0.01	3.16 ± 0.01		
SCR (mm)	H	3.12 ± 0.01	3.11 ± 0.02	3.12 ± 0.03	3.14 ± 0.02	3.17 ± 0.02	3.15 ± 0.01	3.13 ± 0.03	3.14 ± 0.02	3.11 ± 0.02	3.13 ± 0.02
	L	3.16 ± 0.02	3.18 ± 0.02	3.10 ± 0.02	3.10 ± 0.02	3.14 ± 0.02	3.15 ± 0.01	3.11 ± 0.02*	3.13 ± 0.02		
CR (mm)	H	3.14 ± 0.01	3.12 ± 0.01	3.14 ± 0.03	3.16 ± 0.02	3.19 ± 0.02*	3.16 ± 0.01	3.14 ± 0.03	3.15 ± 0.02	3.13 ± 0.02	3.15 ± 0.02
	L	3.18 ± 0.02	3.19 ± 0.02	3.12 ± 0.02	3.12 ± 0.02	3.17 ± 0.02	3.17 ± 0.02	3.12 ± 0.01*	3.14 ± 0.02		
CA (D)	H	−1.21 ± 0.12	−0.91 ± 0.13	−1.62 ± 0.25*	−1.11 ± 0.12	−1.64 ± 0.13***	−0.96 ± 0.13	−1.09 ± 0.12	−0.83 ± 0.09	−1.40 ± 0.14*	−0.97 ± 0.09
	L	−1.47 ± 0.10**	−1.00 ± 0.08	−1.56 ± 0.18*	−1.05 ± 0.10	−1.61 ± 0.12**	−1.09 ± 0.10	−1.06 ± 0.12	−0.89 ± 0.07		
CJ0 (D)	H	−0.48 ± 0.07	−0.43 ± 0.07	−0.71 ± 0.11*	−0.49 ± 0.06	−0.37 ± 0.08	−0.30 ± 0.07	−0.08 ± 0.09	−0.34 ± 0.06	−0.43 ± 0.07	−0.43 ± 0.06
	L	−0.52 ± 0.13	−0.47 ± 0.04	−0.56 ± 0.13	−0.44 ± 0.07	−0.54 ± 0.06	−0.50 ± 0.06	−0.24 ± 0.07	−0.35 ± 0.03		
CJ45 (D)	H	+0.10 ± 0.09	+0.06 ± 0.04	−0.23 ± 0.11*	+0.08 ± 0.07	−0.67 ± 0.07***	+0.09 ± 0.08	−0.33 ± 0.10**	+0.09 ± 0.05	−0.48 ± 0.08***	+0.01 ± 0.05
	L	+0.00 ± 0.09	+0.08 ± 0.04	−0.25 ± 0.10*	+0.08 ± 0.07	−0.55 ± 0.06***	−0.07 ± 0.04	−0.30 ± 0.07**	−0.04 ± 0.06		

Comparisons of six corneal shape parameters were made for treated right eyes (RE) versus the untreated left eyes (LE) by Student's paired t-tests and for fellow untreated left eyes from the −10DS group versus fellow untreated left eyes from the eight sphero-cylindrical lens-wear groups using one-way ANOVA with Bonferroni's post hoc tests. Data for groups treated with sphero-cylindrical lenses were arranged according to the astigmatic axis (45°, 90°, 135°, and 180°) and magnitude (high, H, −6DS/−8DC; low, L, −8DS/−4DC). Data for group treated with spherical lenses (−10DS) are presented on the right for easy comparison. The levels of significance are represented by different symbols: *P < 0.05, **P < 0.01, and ***P < 0.001 for paired t-tests, and †P < 0.05, ††P < 0.01, and †††P < 0.001 for post hoc tests.
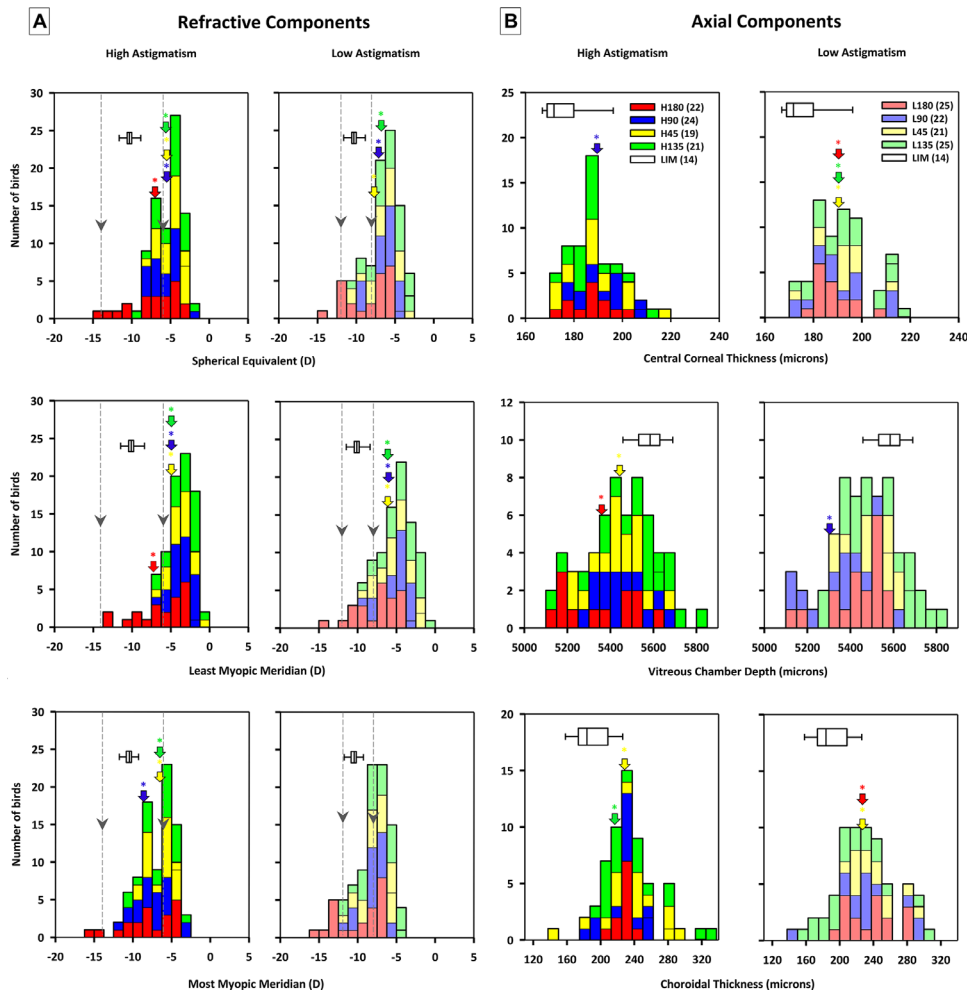
FIGURE 1. Effects of the presence of astigmatism on refractive (**A**) and axial (**B**) components in the treated eyes. Frequency distributions of three refractive (**A**) and axial (**B**) parameters of chicks treated with sphero-cylindrical lenses of two astigmatic magnitudes (high, H; low, L) and four astigmatic axes (45°, *yellow*; 90°, *blue*; 135°, *green*; and 180°, *red*). The *darker* (*left column*) and *lighter* (*right column*) shades represent the higher and lower magnitudes of astigmatism imposed, respectively. The sample size for each group is shown in the parentheses in the legend. In each plot, the horizontal boxplot presents the descriptive statistics (the *solid line* and *box margins* represent the median and interquartile range, respectively) of the group wearing the −10D lens (LIM). Significant differences between LIM with individual sphero-cylindrical lens-wear groups (marked by *colored arrows*) were found in these refractive and axial parameters (one-way ANOVA with Bonferroni-corrected pairwise post hoc comparisons). The level of significance (from LIM) is indicated by *$P < 0.05$.
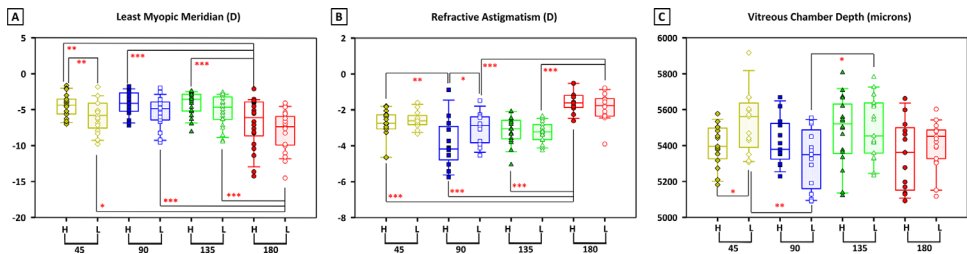

FIGURE 2. Effects of astigmatic magnitude and axis on the least myopic meridian (**A**), refractive astigmatism (**B**), and vitreous chamber depth (**C**) in the treated eyes. Comparisons of three parameters at the end of the treatment period among the eight groups of birds treated with sphero-cylindrical lenses. The eight groups of birds are organized from *left* to *right* according to the magnitude (high, H; low, L) and cylindrical axis (45°, 90°, 135°, and 180°). Each symbol represents data from one bird; the *solid line* in the box and the *box margins* represent the median and interquartile range, respectively, for each group. Significant differences between groups (two-way ANOVA with Bonferroni's multiple post hoc comparisons) are indicated by *$P < 0.05$, **$P < 0.01$, and ***$P < 0.001$. Birds treated with 180 cylindrical axes developed higher LMM (**A**) but lower refractive astigmatism (**B**) compared to birds treated with the other three orientations. In addition, the L90 group had a significantly shorter vitreous chamber depth than the L45 and L135 groups.
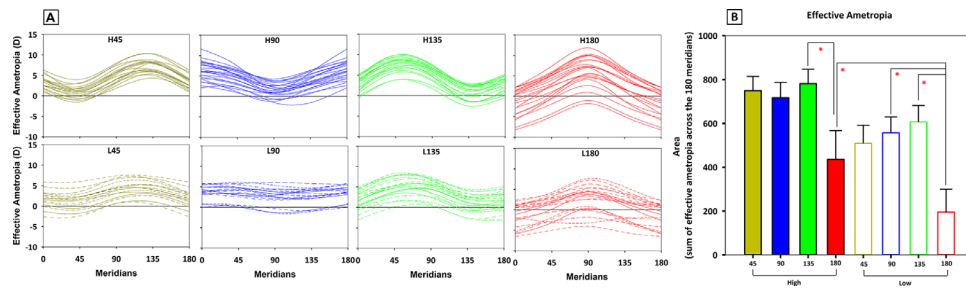
FIGURE 3. Effective ametropia at the end of the treatment period in birds treated with sphero-cylindrical lenses. (**A**) Effective ametropia (ocular ametropia–lens power) as a function of meridian for individual birds (*colored lines*) at the end of the treatment period. Group data are arranged according to cylindrical magnitude (*top*, high magnitude, *solid line*; *bottom*, low magnitude, *dashed line*) and axis (*left to right*: 45°, 90°, 135°, and 180°). In each plot, the *black solid line* represents the emmetropic condition; the area enclosed by each curve (bird) from this *black line* is calculated as an arbitrary unit to quantify the effective ametropia. (**B**) Effective ametropia (mean and SEM), calculated as an area departing from the emmetropic line (summation of effective ametropia [ocular ametropia–lens power] across the 180° meridians), for the eight groups of birds treated with sphero-cylindrical lenses. In general, with the same magnitude of astigmatism imposed (i.e., high or low), birds treated with 180 cylindrical axes developed the lowest effective ametropia compared to the other three groups. Significant differences between groups (two-way ANOVA with Bonferroni's multiple post hoc comparisons) are indicated by *$P < 0.05$.

three groups receiving the same magnitude but different axes (two-way ANOVAs with Bonferroni's multiple post hoc comparisons, all $P \leq 0.05$). In addition, the H180 group also developed significantly lower RA when compared to the other three groups with the same magnitude but different axes (two-way ANOVAs with Bonferroni's multiple post hoc comparisons, all $P \leq 0.001$), whereas the L180 group had significantly lower RA when compared to L90 and L135 groups (two-way ANOVA with Bonferroni's multiple post hoc comparisons, all $P \leq 0.05$). Significant difference in RA was also observed between H90 versus H45 and L90 groups (two-way ANOVAs with Bonferroni's multiple post hoc comparisons, all $P \leq 0.05$). For the vector components, H180 and L180 groups resulted in positive R-J0, which was significantly different from the other three orientations of the same astigmatic magnitude. In contrast, both H135 and L45 developed significantly higher R-J45 than the other three groups of different orientations but with same astigmatic magnitude (two-way ANOVAs with Bonferroni's multiple post hoc comparisons, all $P \leq 0.05$). In addition, R-J45 in the H45 group was significantly higher than those in H180 and H90 groups (two-way ANOVA with Bonferroni's multiple post hoc comparisons, all $P \leq 0.001$), whereas R-J45 in the L135 group was significantly lower than those in H135 and L90 groups (two-way ANOVA with Bonferroni's multiple post hoc comparisons, all $P \leq 0.01$).

To compare the effect of sphero-cylindrical lens wear on emmetropization, Figure 3A shows the effective ametropia profile at the end of the treatment period for individual birds in each group. Using the calculation method from an earlier study involving monkeys,[35] the effective ametropia for individual meridians was derived by subtracting the lens refractive power from the ocular refraction. The refractive power at a given meridian θ is derived by

$$F_\theta = F_{Sph} - F_{Cyl}\sin(\theta - \alpha)^2$$

where F_{Sph} and F_{Cyl} are the spherical and cylindrical powers, respectively, and α is the axis of the minus cylinder. As shown in Figure 3A, imposing a lower magnitude of astigmatism (bottom panel) usually resulted in a smaller effective ametropia (i.e., a smaller departure from emmetropia) when compared to imposing a higher magnitude of astig-

matism (top panel). To quantify the magnitude of departure of effective ametropia from emmetropia as a whole, the area enclosed by the effective ametropia curve and emmetropia (black line in Fig. 3A) was calculated for individual birds and this magnitude compared across groups. Two-way ANOVAs revealed that both the axis ($P < 0.001$) and magnitude ($P < 0.001$) of astigmatism had significant effects on the effective ametropia (area), but no interaction effects were found. As presented in Figure 3B, L180 induced significantly less effective ametropia compared to L90, L135, and H180, whereas H180 had less effective ametropia compared to H135 (two-way ANOVA with Bonferroni's multiple post hoc comparisons, all $P \leq 0.05$).

Axial Parameters. Astigmatic axis produced significant main effects on the vitreous chamber depth (two-way ANOVA, $P < 0.01$), but astigmatic magnitude had no significant effects on axial parameters. Figure 2C shows the effects of astigmatic axis on vitreous chamber depth. The L90 group had shorter vitreous chamber depth when compared to L45 and L135 groups (two-way ANOVAs with Bonferroni's multiple post hoc comparisons, $P < 0.05$). In addition, the H45 group had a significantly shorter vitreous chamber depth when compared to the L45 group (two-way ANOVA with Bonferroni's multiple post hoc comparisons, $P < 0.05$). Among these sphero-cylindrical lens-wear groups, the L135 group showed a thinner choroid when compared to the H135 and L180 groups (two-way ANOVA with Bonferroni's multiple post hoc comparisons, $P < 0.05$). There were no significant differences in the remaining axial components (central corneal thickness [CCT], anterior chamber depth [ACD], lens thickness [LT], retinal thickness [RT], scleral thickness [ST], and axial length [AXL]) among these eight groups of birds.

Corneal Shape Parameters. Astigmatic axis produced significant main effects on corneal astigmatism (two-way ANOVA, $P < 0.001$) and the two vector components (C-J0 and C-J45; both $P < 0.001$). In contrast, astigmatic magnitude had no significant effects on corneal shape parameters. When groups treated with the same magnitude were compared, significantly higher corneal astigmatism was found in birds treated with 135° compared to 180° cylindrical axis (H135 versus H180 and L135 versus L180; two-way ANOVA with Bonferroni's multiple post hoc comparisons, $P < 0.05$; Table 4). For C-J0, the H90 group was

TABLE 5. Correlations Between Refractive Components and Axial Parameters in Different Treatment Groups

| Characteristic | LIM | | | 180 | 90 | 45 |
	LT	VCD	AXL	RT	LT	VCD
M	−0.63*	−0.54*	−0.52*	−0.39*	−0.52**	ns
LMM	−0.57*	−0.55*	ns	−0.41*	−0.49*	−0.40*
MMM	−0.67**	ns	−0.55*	−0.41*	−0.51**	ns

Significant correlations were found between three spherical ametropia (M, LMM, and MMM) and individual axial parameters (LT, VCD, AXL, and RT). The levels of significance (Pearson's correlation coefficient) are represented by *$P < 0.05$ and **$P < 0.01$. ns, nonsignificant.

significantly more negative than the H180 group (two-way ANOVA with Bonferroni's multiple post hoc comparisons, $P < 0.05$). For C-J45, the H135 group had a significantly more negative value compared to the H45, H90, and H180 groups (two-way ANOVA with Bonferroni's multiple post hoc comparisons, all $P < 0.05$). There were no significant differences in the other corneal components.

Correlations Between Refractive, Corneal, and Axial Components

Subsets of birds, which had all biometric parameters measured, were used for correlation analyses. Because the imposed astigmatic magnitude did not produce significant effects on these parameters, the data from both groups (high and low magnitudes) receiving the same astigmatic axis were pooled. Results from these five groups of birds (LIM, 45°, 90°, 135°, and 180°) are presented below.

Refractive and Axial Components. Table 5 presents significant Pearson's correlation coefficients found between refractive and axial parameters. While M and LMM were significantly correlated with vitreous chamber depth (VCD) in LIM (all $P < 0.05$), only LMM was significantly correlated with VCD in birds treated with the cylindrical axis oriented at 45° (all $P < 0.05$). In the LIM group, M and MMM were mildly correlated with axial length (all $P < 0.05$). The three spherical ametropia were significantly correlated with lens thickness in LIM (all $P < 0.05$) and birds treated with 90° cylindrical axis (all $P < 0.05$). In contrast, the three spherical ametropia were significantly correlated with retinal thickness in birds treated with 180° cylindrical axis (all $P < 0.05$). There were no other significant correlations observed between refractive and axial components.

Refractive and Corneal Components. Supplementary Figure S2 shows the results of Pearson's correlation analyses between refractive astigmatism and corneal (top) and internal astigmatisms (bottom). Only correlation coefficients showing statistical significance are inserted in each plot. In general, internal astigmatic components were more strongly correlated with refractive than with corneal components. While refractive and internal astigmatic magnitudes were significantly correlated in all groups (all $P < 0.01$), corneal and refractive astigmatic magnitudes were significantly correlated only in groups treated with 90° and 135° axes (both $P < 0.05$). For J0 and J45 astigmatic components, while refractive and internal components were significantly correlated in all groups (all $P < 0.01$), corneal and refractive J0 were only mildly correlated in groups treated with 90° and 135° axes (both $P < 0.01$). In contrast, the flattest ($r = 0.34$, $P = 0.04$) and mean ($r = 0.33$, $P = 0.05$) corneal curvatures

were correlated with LMM in birds treated with the 135° cylindrical axis. There were no other significant correlations between refractive and corneal components.

Corneal and Axial Components. Both the flattest and steepest corneal radii were correlated with axial length in all ($P < 0.01$) except the 180° cylindrical axis–treated group. In contrast, both corneal radii were correlated with vitreous chamber depth in all groups (all $P < 0.05$). Figure 4 shows the positive correlations between these parameters; only Pearson's r with statistical significance is inserted. The relationship between the ratio of vitreous chamber depth to corneal radius (VCD/CR) and the ratio of axial length to corneal radius (AL/CR) with spherical ametropia was further investigated. Table 6 presents the Pearson's correlation analyses between three spherical ametropia with VCD/CR and AL/CR. In the LIM group, there were no significant correlations between spherical ametropia with either ratio (VCD/CR and AL/CR). All three spherical ametropia were significantly correlated with VCD/FCR (all $P < 0.05$) and VCD/SCR (all $P < 0.05$) in birds treated with 180° and 45° cylindrical axes, and significant correlation was noted with AL/FCR (all $P < 0.05$) and AL/SCR (all $P < 0.05$) in birds treated with 180° and 135° cylindrical axes. There were no other significant correlations between corneal and axial components.

DISCUSSION

Using chicken as an animal model, it was shown that (1) imposing hyperopic-astigmatic defocus induced myopic-astigmatic error in the treated eyes; (2) with the same level of spherical-equivalent hyperopic blur (−10D), the presence of astigmatism in the sphero-cylindrical lens-wear groups induced less myopia than the spherical lens-wear group; and (3) myopia development was sensitive to the magnitude and axis of astigmatic blur.

Effects of Sphero-Cylindrical Lens Wear on Treated and Fellow Untreated Eyes

While wearing −10D spherical lenses induced typical changes in refractive and axial parameters of the treated eyes as previously reported,[41,43] sphero-cylindrical lens wear produced significant refractive (Table 1), axial (Table 2), and corneal changes (Table 3) that depended on the astigmatic characteristics (see further discussion below) in both treated and fellow untreated eyes. The eyes treated with sphero-cylindrical lenses not only developed significantly deeper anterior and vitreous chamber depths, similar to those wearing spherical lenses, but also developed idiosyncratic changes in anterior axial components (e.g., central corneal thickness) and corneal refractive parameters (e.g., steeper corneal radius) in individual groups of birds. Interestingly, the untreated eyes of birds wearing sphero-cylindrical lenses also showed a variety of changes from anterior to posterior segments compared to the untreated eyes of −10D birds (Supplementary Materials section). To the best of our knowledge, this is the first study to report significant impacts of sphero-cylindrical lenses on a wide range of ocular parameters. Although one previous study used a combination of spherical lenses (±3DS and ±6DS) and crossed-cylindrical lenses (+5DS/−10DC) to create a sphero-cylindrical lens effect, comparison with the current study is difficult because the closest match to our lenses was −1DS/−10DC[52] (further discussion below). In this respect, the inclusion of
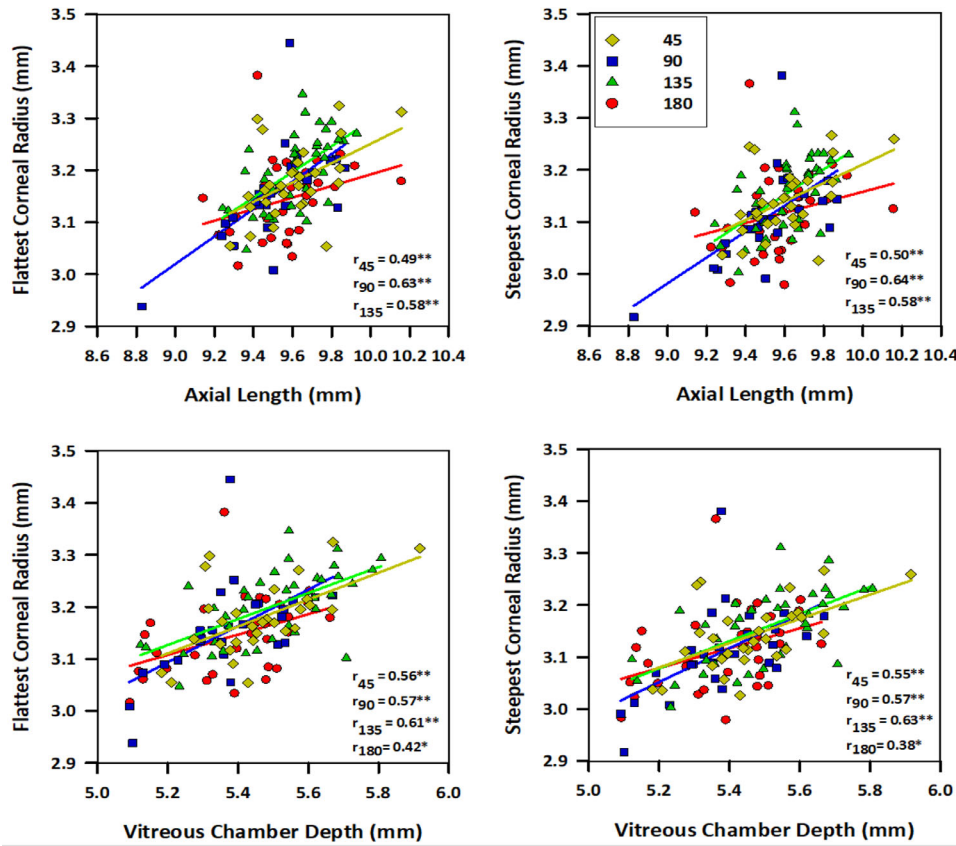
FIGURE 4. Correlations between corneal radius of curvature with axial length and vitreous chamber depth. Corneal radii along the flattest (*left column*) and steepest (*right column*) meridians are plotted against the axial length (*top row*) and vitreous chamber depth (*bottom row*) in eyes treated with sphero-cylindrical lenses of different cylindrical axes. *Different-colored symbols* represent groups receiving different cylindrical axes, as shown in the legends. The significant level of correlation is represented by *$P < 0.05$ and **$P < 0.01$. All except one group showed significant correlations between both corneal radii (flattest and steepest) with axial length and vitreous chamber depth. The only exception was the group treated with 180° axis, in which no correlation was found between both corneal radii with the axial length.

TABLE 6. Correlations Between the Spherical Ametropia With Ratios of VCD/CR and AL/CR in Different Treatment Groups

	45				135			180			
Ratios	VCD/FK	VCD/SK	AL/FK	AL/SK	VCD/FK	VCD/SK	AL/FK	AL/SK			
M	−0.40*	−0.41*	−0.38*	−0.37*	−0.38*	−0.40*	−0.44*	−0.45**			
LMM	−0.38*	−0.39*	−0.40*	−0.37*	−0.37*	−0.39*	−0.43*	−0.44*			
MMM	−0.41*	−0.41*	−0.35*	−0.35*	−0.35*	−0.37*	−0.44*	−0.45**			

Significant correlations were found between three spherical ametropia (M, LMM, and MMM) and ratios of VCD/corneal radii (VCD/FCR, ratio of vitreous chamber depth to flattest corneal curvature; VCD/SCR, ratio of vitreous chamber depth to steepest corneal curvature) and ratios of AL/corneal radii (AL/FCR, ratio of axial length to flattest corneal curvature; AL/SCR, ratio of axial length to steepest corneal curvature). The levels of significance (Pearson's correlation coefficient) are represented by *$P < 0.05$ and **$P < 0.01$.

refractive, axial, and corneal measurements in this study provides a strong foundation for future work in this area. Nevertheless, because children rarely encounter this magnitude of hyperopic-astigmatic blur during the normal course of refractive development, the question remains if these results can be translated into human studies.

Astigmatism Interferes With Myopia Development

Although both spherical and sphero-cylindrical lenses imposed the same magnitude of −10D spherical-equivalent error (Table 1), the coexistence of astigmatic blur in the latter treatment clearly alters refractive and ocular endpoints in

chicks (Fig. 1 and Supplementary Tables S1–S3). In contrast to developing approximately −10D of myopia, as in the spherical lens-wear group, *both* principal refractive meridians in the sphero-cylindrical lens-wear group developed lower magnitudes of myopia equal to or less than the magnitude sufficient to compensate for the least hyperopic image plane (Fig. 1 and Table 1). Comparison of the distributions between the two principal refractive meridians (Fig. 1A, middle versus bottom plots) indicates that, while there are subtle differences between groups (Fig. 1A, arrowheads), overall the most myopic meridian appears to be more successful than the least myopic meridian in developing myopic magnitude that closely matches the image
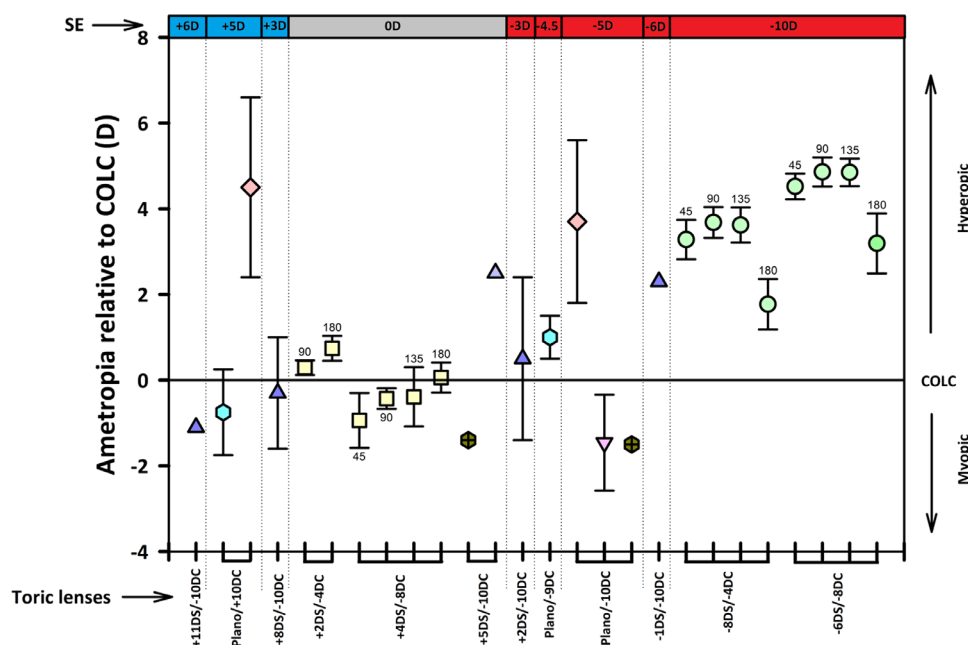
FIGURE 5. Impacts of optically imposed astigmatism on the effective endpoint in chicks. Comparisons of effective endpoints, with respect to the plane of COLC, across different studies. The effective endpoint on the *y*-axis is calculated by subtracting the COLC (*x*-axis, *bottom*: cylindrical format; *x*-axis, *top*: spherical-equivalent format) from the resultant ametropia for individual treatment groups reported in the literature. A positive value indicates a relative hyperopic endpoint and vice versa (*y*-axis, *right*). Different symbols represent different studies; number above the symbol indicates the axis of the cylindrical lens. For each study, the starting day of treatment (e.g., P6, posthatching day 6) and the duration of lens treatment are given for references; ▲, McLean and Wallman, 2003[52]: P6, 2 days; ⬡, Irving et al., 1995[38]: P0/P2, 7 days; ◇, Schmid and Wildsoet, 1997[39]: P0, 12 days; □, Chu and Kee, 2015[42]: P5, 7 days; ▽, Phillips and Collins, 2000[53]: P3, 7 days; ✛, Thibos L, et al. *IOVS* 2001;42:ARVO Abstract 324: P4, 7 days; ○, current study: P5, 7 days. The effective endpoint appears to be directed toward the hyperopic image plane relative to COLC in chicks receiving a high magnitude of hyperopic spherical-equivalent errors (–10D).

plane imposed by the weaker lens meridian (dashed lines on the right in Fig. 1A). Consequently, the average spherical-equivalent values (Fig. 1A, top plots) are more hyperopic than this image plane. Thus, results from all three refractive parameters support the notion that the endpoint is directed toward the least hyperopic image plane in the sphero-cylindrical lens-wear groups.

Whether astigmatism alters the endpoints of refractive development is an important question and has been investigated only in chick and monkey models. Nevertheless, interpreting results across these studies requires caution because different astigmatic magnitude, cylindrical lens design (plano-/crossed-/sphero-cylindrical), and experimental protocols (age of onset, treatment period, axis orientation) were used.[3,45] In contrast to the only monkey study, which used a crossed-cylindrical lens with zero spherical equivalent (+1.50D and −1.50D in the two principal meridians), the chick studies used different lens designs with spherical equivalents ranging from 0D to ±6D (Thibos L, et al. *IOVS* 2001;42:ARVO Abstract 324).[38,39,42,52,53] In order to incorporate this information into the comparison of chick studies, Figure 5 illustrates the effects of imposing astigmatic blur on the resultant ametropia relative to the location of circle of least confusion (COLC), organized along the *x*-axis (top) by the magnitude of spherical equivalent received. Note that the induced ametropia is expressed as a relative value to the COLC plane (i.e., eye's ametropia–lens refraction). Thus, a value closer to zero on the *y*-axis indicates that the refractive endpoint attempts to match the COLC plane, whereas a positive value indicates that the endpoint is more hyperopic than the COLC and vice versa. As shown

in Figure 5, it is clear that the presence of different degrees of spherical equivalent combined with constant astigmatic blurs did not result in extreme myopia similar to that induced by form deprivation conditions,[45] a finding consistent with the monkey study using a relatively large number of animals.[36] Rather, the endpoints in these studies appeared to be directed toward the image plane that were near the COLC plane (Thibos L, et al. *IOVS* 2001;42:ARVO Abstract 324)[38,53] or the more hyperopic plane than COLC.[39,42,52] In this respect, the current study, which involved a relatively large number of chicks, provides the first evidence that in the presence of hyperopic-astigmatic blur, the emmetropization process for both principal refractive meridians is directed toward the least hyperopic image plane (Fig. 1A). These results are supported by the hypothetical optical effects on the astigmatic focal planes in an earlier monkey study[36]: regardless of the pupil size, computations of modulation transfer function (MTF) for a monochromatic point source indicate that the volumes underneath the three-dimensional MTF (taking into account different spatial frequencies and orientations) were much higher at the astigmatic line foci than that at the COLC. Hence, directing the developing retinal plane to the least hyperopic image plane (the closest focal plane) would facilitate the overall neuronal activities with respect to retinal contrast and orientation.

Differential Effects of Astigmatic Orientation on Eye Growth

The axis of astigmatism produced an extensive impact on myopia development (Figs. 2–4, Tables 2–4). Among the

four astigmatic axes tested, ATR (axis 180°) and WTR astigmatism (axis 90°) typically induced differential biometric changes. First, ATR treatment resulted in the highest myopic errors in all three spherical components (M, LMM, and MMM) (Figs. 1, 2 and Table 2). Although there was no significant difference in axial length between ATR and WTR groups, significant correlation of spherical ametropia with the ratio of axial length/corneal curvature was found only in the ATR group (Table 6). Second, WTR treatment induced the highest refractive astigmatism and C-J0 astigmatic component (Fig. 2 and Tables 2, 4). Third, the ATR group showed the least departure from effective emmetropia (Fig. 3B). Fourth, the WTR group induced the least departure from the target astigmatism (Supplementary Fig. S1B). Finally, all except the ATR groups showed significant correlations between corneal radii (flattest and steepest) and axial length (Fig. 4, top panel). These results suggest that the eye growth mechanism in chicks is sensitive to complex visual cues containing spherical and astigmatic errors, resulting in both axial and meridional (i.e., horizontal and vertical) changes. In addition, using similar magnitudes of astigmatic blur (4DC and 8DC) with a spherical-equivalent power of 0 in a recent study, it was observed that WTR treatment induced higher refractive and corneal astigmatisms compared to ATR treatment.[42] Furthermore, the ATR group exhibited asymmetric posterior eye shape (horizontal versus vertical meridians up to 50° eccentricity) that was distinctly different from the WTR and control groups. Interestingly, a similar differential effect was observed in a group of monkeys receiving ATR and WTR astigmatisms in fellow eyes (with alternate occlusion): three of the eight monkeys developed more myopia in ATR-treated eyes when compared to the fellow WTR-treated eyes.[36] In addition, monocularly ATR-treated monkeys showed a bimodal refractive change (Fig. 5 in Kee et al.[36]), consistent with the bimodal distributions of spherical and axial components observed in the current study (Figs. 1A, 1B, red bars), particularly in the ATR-treated group. In humans, while longitudinal studies showed that children with ATR astigmatism at an early age were more likely to develop myopia during school age when compared to those with WTR,[28–30] cross-sectional studies have shown an association of WTR astigmatism with high myopia in the young adult population.[8,31,32,54] Based on the current results, imposing ATR astigmatism (180° axis) together with hyperopic defocus in chicks promoted more myopia with compensatory WTR astigmatism, and imposing WTR astigmatism (90° axis) induced less myopia with compensatory ATR astigmatism, resulting in a pool of chicks with higher myopia more frequently associated with WTR astigmatism (Figs. 1–3 and Supplementary Fig. S1). This observation may explain why WTR astigmatism is more frequently associated with high myopia in human adults.[31] Interestingly, in a longitudinal study[28] that followed up children from birth for >15 years, there is evidence that a larger proportion of children with initial WTR astigmatism shifted to ATR astigmatism than of those with initial ATR astigmatism who shifted to WTR astigmatism (Fig. 4 in Gwiazda et al.[28]). Although the sample sizes were not large (27 and 60, respectively), this result is resonant of what was observed in the current study of chicks, that is, WTR astigmatism induced more compensatory astigmatism than ATR astigmatism (Supplementary Fig. S1). While translating findings from chickens to humans requires caution, regarding their anatomic differences,[45] the availability of this animal model[55] can facilitate further investigations into

the biological effects of early astigmatic subtypes on eye growth.

Why should ATR astigmatism induce more myopia compared to WTR astigmatism? In this study, spherocylindrical lenses of the same magnitude with different axes imposed the same interval of Sturm with line foci of different orientations at different planes (see illustrations in Table 1). In ATR-treated eyes, the horizontal line of focus was displaced farther away from the retina (posterior plane) than the vertical line of focus (anterior plane), while WTR-treated eyes encountered the opposite effects. As shown in Fig. 1A, most birds wearing sphero-cylindrical lenses developed refractive errors compensatory to the anterior focal plane, while the ATR group had only a few birds (red bar) that developed myopia strong enough to fully compensate the posterior focal plane. One possible explanation for this finding is that, despite the increased variability in refractive endpoint, probably due to the deficient signaling pathway in the presence of chronic astigmatic blur, a focal plane containing horizontal (WTR case) or near-horizontal line focus (oblique cases) closer to retina may be more potent in directing the outcome of refractive development. For this hypothesis to work, evidence that supports an orientation-dependent eye growth system is needed. In this regard, previous studies have shown that our visual systems are tuned to horizontal or vertical orientation over oblique,[56–58] an effect termed *oblique effect*.[59] Several visual functions in humans, including spatial acuity,[60] contrast sensitivity,[22,58] vernier acuity,[61] and orientation discrimination,[62] also exhibited similar orientation preferences. Although the oblique effect is known to affect the visual performance at different meridians,[63] whether and how the developing visual system operates with a preferred orientation remains elusive. Another possibility is that the deficient signaling pathway is operating with the principle of optimizing image qualities at both focal planes (either simultaneously or alternately in time domain), which would require concerted efforts of axial and meridional changes. The findings that all except the ATR group showed statistically significant correlations between corneal radii (flattest and steepest) with axial length (Fig. 4, top panel) seems to support this hypothetical model. It is possible that the ATR group was somehow constrained by this coordinative structural change in axial and corneal components.

Structural Correlates in Myopic-Astigmatic Development

In this study, the induced refractive astigmatism was more strongly correlated with internal ($r = 0.45$ to 0.60) than with corneal astigmatism ($r = 0.33$ to 0.48) (Supplementary Fig. S2). Using crossed-cylindrical lenses of similar astigmatic magnitudes with spherical equivalent of 0D in a recent study, a higher correlation of refractive and internal astigmatism in chicks was also noted.[42] In that study, both refractive and internal astigmatisms were correlated with posterior eye shape parameters, including equatorial diameters and ocular expansions at different regions.[42] It has been proposed that the lack of off-axis astigmatism and the superior visual performance at far peripheral visual field in chickens were attributable to an internal refractive component, such as the crystalline lens, but not corneal shape.[64] Given the results from the current and previous studies, further investigations are needed to investigate the contribution of internal ocular

structures to the induced astigmatism in myopic-astigmatic eyes.

An unexpected structural change in the myopic-astigmatic eyes was the thicker choroid (see Table 3 and Supplementary Table S2). While all sphero-cylindrical lens-wear groups showed a thicker choroid compared to the LIM group, these differences reached a statistically significant level in ATR-treated (H180 and L180), 45°-treated (H45 and L45), and 135°-treated (H135) groups. It should be noted that neither meridian of sphero-cylindrical lenses imposed myopic defocus, which is an optical cue consistently found to induce choroidal thickening in animals, including chickens, monkeys, and humans.[45] In a recent human study, imposing WTR and ATR astigmatic blurs using a plano/+3.00DC cylindrical lens (unlike our study, the line focus due to a +3.00D lens was in front of retina) induced bidirectional changes in choroidal thickness within 60 minutes, although the magnitudes of change were not as great as those induced by equivalent spherical defocus.[65] These results provide further evidence that the mechanism regulating refractive development is sensitive to astigmatic defocus in chicks and humans. Thus, it would be of interest to investigate the role of these choroidal changes in inhibiting the myopia induced by LIM.

Limitation of Current Study

To the best of our knowledge, this is the first study to investigate the impacts of early astigmatism on myopia, using a relatively large sample of chickens. However, two limitations of this study do caution its interpretation. First, the influence of the astigmatism was assessed only after 7 days of treatment. Several studies have shown that chicks are capable of developing compensatory eye growth to spherical defocus as high as 10D within a week. While the LIM group showed typical ocular parametric changes compensatory to the −10D defocus and the sphero-cylindrical lens-wear groups showed various endpoints according to the treatment lenses (Fig. 3B), the possibility that the compensation would differ if a longer treatment period was employed cannot be excluded. Second, the impacts of hyperopic-astigmatic defocus of two magnitudes combined with four axes were measured at a single time point. Further longitudinal studies are needed to determine the progress of the effects of different combinations of astigmatic defocus (including myopic-astigmatic) on eye growth.

CONCLUSIONS

Astigmatic magnitude and axis can alter the endpoint of myopia development. The axial and refractive changes found at both anterior and posterior segments indicate a more complex eye growth mechanism in myopic-astigmatic eyes. Although high intersubject variability in refractive development was noted in all sphero-cylindrical lens-wear groups, the extremely high myopia commonly found under form-deprived conditions did not occur, suggesting the involvement of a closed-loop neural feedback system. These results provide foundation work on myopic-astigmatic development in a common animal model and open the possibility to control abnormal refractive development by optical interventions.

References

1. Lyle W. *Astigmatism. Refractive Anomalies Research and Clinical Applications.* Boston: Butterworth-Heinemann; 1991:146–173.
2. Read SA, Collins MJ, Carney LG. A review of astigmatism and its possible genesis. *Clin Exp Optom.* 2007;90:5–19.
3. Kee CS. Astigmatism and its role in emmetropization. *Exp Eye Res.* 2013;114:89–95.
4. He M, Zeng J, Liu Y, Xu J, Pokharel GP, Ellwein LB. Refractive error and visual impairment in urban children in southern china. *Invest Ophthalmol Vis Sci.* 2004;45:793–799.
5. Shih YF, Hsiao CK, Tung YL, Lin LL, Chen CJ, Hung PT. The prevalence of astigmatism in Taiwan schoolchildren. *Optom Vis Sci.* 2004;81:94–98.
6. Fan DS, Rao SK, Cheung EY, Islam M, Chew S, Lam DS. Astigmatism in Chinese preschool children: prevalence, change, and effect on refractive development. *Br J Ophthalmol.* 2004;88:938–941.
7. Leung TW, Lam AK, Deng L, Kee CS. Characteristics of astigmatism as a function of age in a Hong Kong clinical population. *Optom Vis Sci.* 2012;89:984–992.
8. Leung T-W, Lam AK-C, Deng L, Kee CS. Characteristics of astigmatism as a function of age in a Hong Kong clinical population. *Optom Vis Sci.* 2012;89:984–992.
9. Villarreal GM, Ohlsson J, Cavazos H, Abrahamsson M, Mohammed JH. Prevalence of myopia among 12- to 13-year-old schoolchildren in northern Mexico. *Optom Vis Sci.* 2003;80:369–373.
10. Pokharel GP, Negrel AD, Munoz SR, Ellwein LB. Refractive Error Study in Children: results from Mechi Zone, Nepal. *Am J Ophthalmol.* 2000;129:436–444.
11. Kalikivayi V, Naduvilath TJ, Bansal AK, Dandona L. Visual impairment in school children in southern India. *Indian J Ophthalmol.* 1997;45:129–134.
12. Villarreal MG, Ohlsson J, Abrahamsson M, Sjöström A, Sjöstrand J. Myopisation: the refractive tendency in teenagers. Prevalence of myopia among young teenagers in Sweden. *Acta Ophthalmol Scand.* 2000;78:177–181.
13. Kleinstein RN, Jones LA, Hullett S, et al. Refractive error and ethnicity in children. *Arch Ophthalmol.* 2003;121:1141–1147.
14. Huynh SC, Kifley A, Rose KA, Morgan I, Heller GZ, Mitchell P. Astigmatism and its components in 6-year-old children. *Invest Ophthalmol Vis Sci.* 2006;47:55–64.
15. Huynh SC, Kifley A, Rose KA, Morgan IG, Mitchell P. Astigmatism in 12-year-old Australian children: comparisons with a 6-year-old population. *Invest Ophthalmol Vis Sci.* 2007;48:73–82.
16. Wu JF, Bi HS, Wang SM, et al. Refractive error, visual acuity and causes of vision loss in children in Shandong, China. The Shandong Children Eye Study. *PLoS One.* 2013;8:e82763.
17. Kim YS, Lee SY, Park SH. Longitudinal changes in refractive error in a pediatric referral population in Korea. *J Pediatr Ophthalmol Strabismus.* 2017;54:43–51.
18. Lam CS, SH W. Astigmatism among Chinese school children. *Clin Exp Optom.* 1991;74:146–150.

Investigative Ophthalmology & Visual Science

19. Flitcroft DI, Adams GG, Robson AG, Holder GE. Retinal dysfunction and refractive errors: an electrophysiological study of children. *Br J Ophthalmol*. 2005;89:484–488.

20. Abrahamsson M, Sjostrand J. Astigmatic axis and amblyopia in childhood. *Acta Ophthalmol Scand*. 2003;81:33–37.

21. Huang D, Chen X, Zhu H, et al. Prevalence of amblyopia and its association with refraction in Chinese preschool children aged 36–48 months. *Br J Ophthalmol*. 2018;102:767–771.

22. Mitchell DE, Freeman RD, Millodot M, Haegerstrom G. Meridional amblyopia: evidence for modification of the human visual system by early visual experience. *Vis Res*. 1973;13:535–558.

23. Dobson V, Miller JM, Harvey EM, Mohan KM. Amblyopia in astigmatic preschool children. *Vis Res*. 2003;43:1081–1090.

24. Harvey EM, Dobson V, Miller JM, Clifford-Donaldson CE. Amblyopia in astigmatic children: patterns of deficits. *Vis Res*. 2007;47:315–326.

25. Pan CW, Chen X, Gong Y, et al. Prevalence and causes of reduced visual acuity among children aged three to six years in a metropolis in China. *Ophthalmic Physiol Opt*. 2016;36:152–157.

26. Harvey EM, Dobson V, Miller JM, Clifford-Donaldson CE. Changes in visual function following optical treatment of astigmatism-related amblyopia. *Vis Res*. 2008;48:773–787.

27. Harvey EM, Miller JM, Dobson V, Clifford CE. Prescribing eyeglass correction for astigmatism in infancy and early childhood: a survey of AAPOS members. *J AAPOS*. 2005;9:189–191.

28. Gwiazda J, Grice K, Held R, McLellan J, Thorn F. Astigmatism and the development of myopia in children. *Vis Res*. 2000;40:1019–1026.

29. Hirsch MJ. Predictability of refraction at age 14 on the basis of testing at age 6—interim report from the Ojai Longitudinal Study of Refraction. *Optom Vis Sci*. 1964;41:567–573.

30. Grosvenor T, Perrigin DM, Perrigin J, Maslovitz B. Houston Myopia Control Study: a randomized clinical trial. Part II. Final report by the patient care team. *Am J Optom Physiol Opt*. 1987;64:482–498.

31. Farbrother JE, Welsby JW, Guggenheim JA. Astigmatic axis is related to the level of spherical ametropia. *Optom Vis Sci*. 2004;81:18–26.

32. Mandel Y, Stone RA, Zadok D. Parameters associated with the different astigmatism axis orientations. *Invest Ophthalmol Vis Sci*. 2010;51:723–730.

33. Howland HC. Infant eyes: optics and accommodation. *Curr Eye Res*. 1982;2:217–224.

34. Charman WN. Myopia, posture and the visual environment. *Ophthalmic Physiol Opt*. 2011;31:494–501.

35. Kee CS, Hung LF, Qiao Y, Smith EL, III. Astigmatism in infant monkeys reared with cylindrical lenses. *Vis Res*. 2003;43:2721–2739.

36. Kee CS, Hung LF, Qiao-Grider Y, Roorda A, Smith EL, III. Effects of optically imposed astigmatism on emmetropization in infant monkeys. *Invest Ophthalmol Vis Sci*. 2004;45:1647–1659.

37. Irving EL, Callender MG, Sivak JG. Inducing myopia, hyperopia, and astigmatism in chicks. *Optom Vis Sci*. 1991;68:364–368.

38. Irving E, Callender M, Sivak J. Inducing ametropias in hatchling chicks by defocus—aperture effects and cylindrical lenses. *Vis Res*. 1995;35:1165–1174.

39. Schmid KL, Wildsoet CF. Natural and imposed astigmatism and their relation to emmetropization in the chick. *Exp Eye Res*. 1997;64:837–847.

40. Shih YF, Ho TC, Chen MS, Lin LL, Wang PC, Hou PK. Experimental myopia in chickens induced by corneal astigmatism. *Acta Ophthalmol*. 1994;72:597–601.

41. Kee CS, Deng L. Astigmatism associated with experimentally induced myopia or hyperopia in chickens. *Invest Ophthalmol Vis Sci*. 2008;49:858–867.

42. Chu CH, Kee CS. Effects of optically imposed astigmatism on early eye growth in chicks. *PLoS One*. 2015;10:e0117729.

43. Irving E, Sivak J, Callender M. Refractive plasticity of the developing chick eye. *Ophthalmic Physiol Opt*. 1992;12:448–456.

44. Kee CS, Marzani D, Wallman J. Differences in time course and visual requirements of ocular responses to lenses and diffusers. *Invest Ophthalmol Vis Sci*. 2001;42:575–583.

45. Troilo D, Smith EL, Nickla DL, et al. IMI–Report on experimental models of emmetropization and myopia. *Invest Ophthalmol Vis Sci*. 2019;60:M31–M88.

46. Schaeffel F, Hagel G, Eikermann J, Collett T. Lower-field myopia and astigmatism in amphibians and chickens. *J Opt Soc Am A Opt Image Sci Vis*. 1994;11:487–495.

47. Wallman J, Adams JI. Developmental aspects of experimental myopia in chicks: susceptibility, recovery and relation to emmetropization. *Vis Res*. 1987;27:1139–1163.

48. Chu CH, Zhou Y, Zheng Y, Kee CS. Bi-directional corneal accommodation in alert chicks with experimentally-induced astigmatism. *Vis Res*. 2014;98:26–34.

49. Nickla DL, Wildsoet C, Wallman J. Visual influences on diurnal rhythms in ocular length and choroidal thickness in chick eyes. *Exp Eye Res*. 1998;66:163–181.

50. Kang BS, Wang L-K, Zheng Y-P, Guggenheim JA, Stell WK, Kee CS. High myopia induced by form deprivation is associated with altered corneal biomechanical properties in chicks. *PLoS One*. 2018;13:e0207189.

51. Thibos LN, Wheeler W, Horner D. Power vectors: an application of Fourier analysis to the description and statistical analysis of refractive error. *Optom Vis Sci*. 1997;74:367–375.

52. McLean RC, Wallman J. Severe astigmatic blur does not interfere with spectacle lens compensation. *Invest Ophthalmol Vis Sci*. 2003;44:449–457.

53. Phillips J, Collins A. Response of the chick eye to simple hyperopic astigmatic defocus. In: *Proceedings of the VIII International Conference on Myopia*; 2000:162–165.

54. Heidary G, Ying G-S, Maguire MG, Young TL. The association of astigmatism and spherical refractive error in a high myopia cohort. *Optom Vis Sci*. 2005;82:244–247.

55. Wisely CE, Sayed JA, Tamez H, et al. The chick eye in vision research: an excellent model for the study of ocular disease. *Prog Retin Eye Res*. 2017;61:72–97.

56. Hubel DH, Wiesel TN. Receptive fields of single neurones in the cat's striate cortex. *J Physiol*. 1959;148:574.

57. De Valois RL, Yund EW, Hepler N. The orientation and direction selectivity of cells in macaque visual cortex. *Vis Res*. 1982;22:531–544.

58. Campbell FW, Kulikowski JJ. Orientational selectivity of the human visual system. *J Physiol*. 1966;187:437–445.

59. Appelle S. Perception and discrimination as a function of stimulus orientation: the" oblique effect" in man and animals. *Psychol Bull*. 1972;78:266.

60. Berkley MA, Kitterle F, Watkins DW. Grating visibility as a function of orientation and retinal eccentricity. *Vis Res*. 1975;15:239–244.

61. Westheimer G, Beard BL. Orientation dependency for foveal line stimuli: detection and intensity discrimination, resolution, orientation discrimination and vernier acuity. *Vis Res*. 1998;38:1097–1103.

62. Mustillo P, Francis E, Oross III S, Fox R, Orban GA. Anisotropies in global stereoscopic orientation discrimination. *Vis Res*. 1988;28:1315–1321.

63. Charman W, Voisin L. Astigmatism, accommodation, the oblique effect and meridional amblyopia. *Ophthalmic Physiol Opt*. 1993;13:73–81.

64. Maier FM, Howland HC, Ohlendorf A, Wahl S, Schaeffel F. Lack of oblique astigmatism in the chicken eye. *Vis Res*. 2015;109:68–76.

65. Hoseini-Yazdi H, Vincent SJ, Read SA, Collins MJ. Astigmatic defocus leads to short-term changes in human choroidal thickness. *Invest Ophthalmol Vis Sci*. 2020;61:48.